EUROPEAN ORGANIZATION FOR NUCLEAR RESEARCH

L3 Note 2677
July 10, 2001

The analysis of $\pi^+\pi^-\pi^0$ production in Two-Photon Collisions

L3 Collaboration

Abstract

The reaction $\gamma\gamma \to \pi^+\pi^-\pi^0$ has been studied with the L3 detector at LEP. The data sample corresponds to a total integrated luminosity of 682.6 pb^{-1} collected at the centre-of-mass energies from 183 GeV to 209 GeV. Preliminary results of the full energy dependent partial wave analysis in the mass region 0.65 - 2.15 GeV are presented. The reaction is dominated by the $a_2(1320)$ formation. Several other signals are also observed.

Submitted to *International Europhysics Conference High Energy Physics 2001*
Budapest, Hungary, 12-18 July 2001.

1 Introduction

Two-photon interactions provide an important tool for the investigation of hadronic states. The two-photon width, $\Gamma_{\gamma\gamma}$, is related to the flavour content of $q\bar{q}$ states and the measurement of form factors provide important informations about the wave function of the quarks inside the meson. Smaller values of $\Gamma_{\gamma\gamma}$ are indication for the presence of a glueball or hybrid components in the state.

The $\gamma\gamma \to \pi^+\pi^-\pi^0$ production has been investigated by several experiments [1, 2], using virtual photons produced in e^+e^- storage rings. In a previous publication L3 [3] has analysed data at centre-of-mass energy $\sqrt{s}\simeq$ 91 GeV for an integrated luminosity L_{ee}=140.6 pb^{-1} obtaining 793 $e^+e^- \to e^+e^-\pi^+\pi^-\pi^0$ events with $(\Sigma\vec{p_T})^2 \leq 0.001$ GeV^2. In this report we present a preliminary analysis of a data sample of 22400 events, taken during the years 1997 to 2000 at LEP, for $\sqrt{s}$= 183 - 209 GeV and L_{ee}= 682.6 pb^{-1}.

A spin-parity analysis is performed on the 1998 data, a sample of 7740 events, corresponding to L_{ee}= 176.7 pb^{-1}. Two photons only couple to states with positive C-parity. The three pion final state has negative G-parity, $G = Ce^{i\pi I_z}$, and thus only I=1 $q\bar{q}$ states can be produced. The spin-parity analysis consider the formation of resonances, R, with $J^P = 0^-, 2^+$ and 2^-, the spin-1 states being forbidden by the Landau-Yang theorem [4] for quasi-real photons. A two-body decay is assumed: $\gamma\gamma \to \mathrm{R} \to \mathrm{R}'\pi$. Only S- and D-wave resonances are considered for R$'$. Due to the conservation of C-parity in neutral decay modes only f-states are produced in the $\pi^+\pi^-$ channel while only ρ-states appear in the $\pi^\pm\pi^0$ channels. We include in the analysis the $f_0(400-1200)$, named σ, the $f_2(1270)$ and the $\rho(770)$.

To describe the two-photon resonance formation the EGPC [5] Monte Carlo generator is used. It describes the two-photon process as the product of the luminosity function, $L_{\gamma\gamma}$, for transverse photon flux [6] and the resonance production cross section:

$$\sigma(\gamma\gamma \to R) = \frac{8\pi(2J+1)M^2\Gamma_{\gamma\gamma}\Gamma}{W^2_{\gamma\gamma}\left[(M^2 - W^2_{\gamma\gamma})^2 + (M\Gamma)^2\right]}, \tag{1}$$

where J is the spin, M the mass and Γ the width of the resonance R; $W_{\gamma\gamma}$ is the two-photon centre-of-mass energy. The Monte Carlo generates the resonance with $\Gamma_{\gamma\gamma}$=1 keV, so the ratio of the measured cross section to that obtained by the Monte Carlo integration gives the measured value of $\Gamma_{\gamma\gamma}$. The decay of the resonance is generated according to Lorentz invariant phase-space. Events are generated for all the resonances of interest and passed through the L3 detector simulation based on the GEANT [7] and GEISHA [8] programs. Time dependent detector inefficiencies, as monitored during the data taking period, are also simulated.

2 Data selection and cross-sections

The L3 detector [9] is suitable for the study of two-photon processes since events with few tracks and low visible energy in the detector are selected by a track trigger [10] with a low threshold on the track transverse momentum, $p_T > 150$ MeV.

The charged pions are measured in the central tracker in the polar angle $13^o \leq \theta \leq 167^o$. The photons are detected by the electromagnetic calorimeter in the barrel region, $42^o \leq \theta \leq 138^o$, and the forward and backward regions, $11.6^o \leq \theta \leq 38^o$.

For quasi-real photons interactions the $e^\pm$ in the final state are mainly scattered at very small polar angles and go undetected. The $e^+e^- \to e^+e^-\pi^+\pi^-\pi^0$ events are selected by requiring two tracks with opposite charge and two isolated electromagnetic clusters.

- The two tracks must be consistent with particles coming from the primary vertex and their dE/dx measurement must correspond to the π hypothesis with a confidence level CL(π) > 10%.
- A photon is an electromagnetic cluster with energy greater than 80 MeV and no nearby tracks in a cone of 0.2 rad half angle. To exclude photons near the edges of the detector a fiducial cut $14^o \leq \theta \leq 35^o$ and $45^o \leq \theta \leq 135^o$ is applied. The $\gamma\gamma$ mass spectrum is presented in Fig.1.
- The π^0 reconstructed is required to have a mass inside 105 MeV $\leq m(\gamma\gamma) \leq$ 165 MeV .

The background in $\gamma\gamma \rightarrow \pi^+\pi^-\pi^0$ is mainly due to inclusive two-photon events. To suppress this background a cut on the total transverse momentum is applied, $(\Sigma\vec{p_T})^2 \leq 0.02$ GeV^2. The $\pi^+\pi^-\pi^0$ effective mass spectra for $(\Sigma\vec{p_T})^2$ below and above the cut are shown in Fig.2. For low $(\Sigma\vec{p_T})^2$ values, i.e. for quasi-real photons, the distribution is dominated by the $a_2(1320)$. At high $(\Sigma\vec{p_T})^2$ values the spin-2 resonance is suppressed, while we observe a signal of $\eta(550)$ and $\omega(782)$. The production mechanism of the $\omega(782)$ is under investigation: a 1^{--} state could be produced in association with other undetected particles, or by a bressthralung process where a virtual photon converts into a vector meson [11].

The $\pi^\pm\pi^0$ mass spectrum is dominated by the $\rho(770)$ as shown in (Fig. 3 upper plot).The $a_2(1320)$ is enhanced when the decay $a_2(1320) \rightarrow \rho\pi$ is selected by requiring that at least one of the $\pi^\pm\pi^0$ mass combinations lie below 1020 MeV(Fig. 3 lower plot).

The $a_2(1320)$ resonance is fitted by a Breit-Wigner plus a third order polynomial background. The mass and width are found to be $M = 1.332 \pm 0.002$ GeV and $\Gamma = 114.8 \pm 3.9$ MeV Fig. 4.

The cross section of the reaction $\gamma\gamma \rightarrow \pi^+\pi^-\pi^0$ is obtained as a function of $W_{\gamma\gamma}$ as

$$\sigma_{\gamma\gamma}(i) = \frac{N(i)}{L_{ee}\Delta L_{\gamma\gamma}\varepsilon(i)}, \tag{2}$$

where $N(i)$ is the number of events observed in a $W_{\gamma\gamma}$ bin i, $\Delta L_{\gamma\gamma}$ is the two-photon luminosity integrated over this bin, $\varepsilon(i)$ is the detection efficiency and L_{ee} the integrated data luminosity. For $L_{\gamma\gamma}$ the equivalent photon approximation is used [6].

The efficiency $\varepsilon(i)$ is determined in each bin by the simulation of the detector acceptance, efficiency and trigger. It varies from 30% to 70% in the region of interest. The comparison of our cross section and the one obtained by ARGUS [2] is shown in Fig. 5. A good agreement is observed, except in the region around 1.1 GeV.

3 Full energy partial wave analysis

The spin-parity analysis based on the approach suggested in [12] is used in the analysis of 7740 events of 1998 data. It is performed on the $\gamma\gamma \rightarrow \pi^+\pi^-\pi^0$ data, with the cut $(\Sigma\vec{p_T})^2 \leq 0.02$ GeV^2 to select events with quasi real photons. The model assumes the formation of resonances which decay in two-body, $\gamma\gamma \rightarrow \mathrm{R} \rightarrow \mathrm{R}'\pi$ and $\mathrm{R}' \rightarrow \pi\pi$. The dominant feature of the $\gamma\gamma$ mass distribution is the formation of the $a_2(1320)$ resonance, but it is also clear in Fig. 5 that we have to include more states in order to describe the regions below and above the $a_2(1320)$. Many states in the mass region higher 2 GeV [13] are expected, but the statistics of the data is quite low. The fitted mass region is restricted to below 2.15 GeV to suppress uncontrolled contributions from tails of high mass states.

The $\pi^{\pm}\pi^0$ mass projection is dominated by the ρ mass as shown in and there is a very small contribution from two pion masses higher than 1600 MeV. We therefore neglect the production of $\rho(1700)$ and $\rho_3(1690)$. The mass distribution in the $\pi^+\pi^-$ spectrum, Fig. 6b, shows very little structure: there are no clear signals from $f_0(980)$, $f_0(1500)$ or $f_2(1275)$. The distribution has a peak around 800 MeV which has a pure kinematical origin, it is the reflection of the $a_2(1320)$ decay into $\rho^{\pm}(770)\pi^{\mp}$. In the spin-parity analysis we considered the following resonances in the $\pi^+\pi^-$ channel: σ, $f_0(980)$, $f_2(1275)$ and $f_0(1500)$. The contributions of the $f_0(980)$ and $f_0(1500)$ are quite small, they are omitted in the final solution, but they are used to verify the stability of the fit. The σ-resonance, i.e. $f_0(400-1200)$, is a parametrisation of the broad component in the S-wave $\pi\pi$-amplitude. This component covers a rather large mass region and an additional $\sigma * s$ term is necessary to reproduce the $\pi\pi$ data [14].

An experimental background approximated as a phase space, is also included in the analysis. Its contribution is constrained to be 10%. A variation of background from 5 % to 15% doesn't affect the results.

3.1 The method

The amplitude for the resonance production is written as:

$$A = \sum_i \epsilon_\mu^{(1)} \epsilon_\nu^{(2)} A^i_{\mu\nu}, \tag{3}$$

where $\varepsilon_\mu^{(1)}$ and $\varepsilon_\nu^{(2)}$ are the polarisation vectors of the photons (1) and (2). The index i corresponds to the three spin states of the two-photon system.

The cross section for the two-photon transition into $\pi^+\pi^-\pi^0$ system, in the $\gamma\gamma$ centre-of-mass, is:

$$d\sigma = \frac{(2\pi)^4}{2s} |A|^2 d\Phi(k_1, k_2, k_3) \tag{4}$$

k_i are the four-momenta of the three-pion system. Background is the nonresonant contribution, approximated by the phase space.

The three $\gamma\gamma$ spin state amplitudes are orthogonal to each other, thus

$$|A|^2 = \sum_{ij} \sum_{kl} \epsilon_\mu^{(1)}(k) \epsilon_\nu^{(2)}(l) A^i_{\mu\nu} \epsilon_\xi^{(1)}(k) \epsilon_\tau^{(2)}(l) A^{j*}_{\xi\tau} = \sum_i g^{\perp\perp}_{\mu\xi} g^{\perp\perp}_{\nu\tau} A^i_{\mu\nu} A^{i*}_{\xi\tau}, \tag{5}$$

with the orthogonality condition:

$$g^{\perp\perp}_{\mu\xi} g^{\perp\perp}_{\nu\tau} A^i_{\mu\nu} A^{j*}_{\xi\tau} = 0 \qquad \text{for} \qquad i \neq j \tag{6}$$

The energy part of the amplitude is parametrised as a sum of Breit-Wigner resonances:

$$A(W^2_{\gamma\gamma}, L_k, L_m) = \sum_i \frac{g_{ik}\Lambda_{im}}{M_i^2 - W^2_{\gamma\gamma} - iM_i\Gamma_i} \frac{1}{\sqrt{F(q, r, L_k) F(k^\perp, r, L_m)}}. \tag{7}$$

Such amplitude describes the transition via the resonance R from a $\gamma\gamma$ state, denoted by index k, with orbital momentum L_k into a meson state m with orbital momentum L_m. In the current analysis we used fixed to [13] values of the resonance parameters M_R and Γ_R. The $F(q, r, L)$ are centrifugal barrier factors with an interaction radius r fixed to 0.8 fm for all resonances. The coupling of the resonance with the $\gamma\gamma$ system g_{ik} should be a real number unless there is a strong interference between resonances. The Λ_{ik} parameters are complex numbers. The imaginary part of a coupling in the Breit-Wigner parametrisation can absorb a part of the non resonant contribution of the amplitude. Thus, if there are two or three resonances in the channel it is not usually necessary to introduce a nonresonant contribution. However in the case of one resonance parametrisation the nonresonant contribution can be important and we introduce it in the 0^{-+} channel.

From the four-vectors of each event we construct a likelihood function L:

$$lnL = \sum_k P_k, \tag{8}$$

where for the event k the P_k is probability derived from the $|A|^2$ (formula 5) and normalised to 1. The summation extends over all measured events. The parameters are fitted to maximise the likelihood function.

To compare the model with the experimental distributions, three mass and three angle distributions are studied:

- the $\pi^+\pi^-\pi^0$, $\pi^-\pi^+$ and $\pi^\pm\pi^0$ masses
- the cosine of the π^0 and $\pi^\pm$ polar angle in the $\gamma\gamma$ centre-of-mass
- the cosine of the $\pi^\pm$ polar angle in the $\pi^+\pi^-$ centre-of-mass

3.2 Results

Many models have been considered in the spin-parity analysis. Starting from the $a_2(1320)$ + BG only hypothesis, which gives $L = -1370$ with 2 parameters fit we have included more and more waves in order to have a satisfactory description of the data over the whole mass range . The check was done by calculating the value of the $\chi^2/d.o.f$ for the independent mass and angular distributions in three $\pi^+\pi^-\pi^0$ mass regions : $1200 - 1400$ MeV, $1400 - 1700$ MeV and $1700 - 1900$ MeV. The best overall solution was found for the following hypothesis: two $J^{PC} = 0^{-+}$ states, two $J^{PC} = 2^{++}$ states and one $J^{PC} = 2^{-+}$ state, presented in Table 1. The Likelihood function for the best fit is equal to – 5512 with 26 parameters fit. The three masses and the three angular distributions are well described, as shown in Fig.6. The $\chi^2/d.o.f$ value is 0.69 for the mass spectra and 1.66 for the angular distributions. The $\pi\pi$ mass distributions for the three $\pi^+\pi^-\pi^0$ mass regions are shown in Fig.7. We discuss here the most significant states seen in this analysis.

- $a_2(1320)$

  This is the strongest resonance in the data and actually defines the main shape of the distribution. It is produced dominantly from the helicity two, ${}^5S_2$, $\gamma\gamma$ state and decays dominantly into $\rho(770)\pi$ with orbital angular momentum $L = 2$. The ratio for the production of the resonance from ${}^5S_2$ and the helicity zero, ${}^1D_2$, $\gamma\gamma$ state is

$$\frac{\sigma(\gamma\gamma({}^5S_2) \to a_2(1320))}{\sigma(\gamma\gamma({}^1D_2) \to a_2(1320))} = 9.1 \pm 0.8 \tag{9}$$

  The ratio of $\gamma\gamma$ couplings is

$$R(\Gamma_{\gamma\gamma}({}^5S_2)/\Gamma_{\gamma\gamma}({}^1D_2)) = 1.20 \pm 0.25$$

consistent with the theoretical prediction [16] $R(^5S_2/^1D_2) = 0.95 \pm 0.15$ for a state with radius 0.6-0.8 fm. The cross-section, derived from the amplitudes obtained in the spin-parity analysis, taking into account the detector efficiencies and the luminosity as in equation 2, is presented in Fig. 8. The difference into efficiencies for each wave are taken into account. The contribution of this resonance into the cross section is 55.7 % quite stable in all fits. The $\gamma\gamma$ partial width is defined with high accuracy and it is given in Table 1.

- $\pi_0(1300)$

  The mass region around 1.3 GeV can not be satisfactory described without a contribution from the pseudoscalar state $\pi(1300)$. The contribution of this state is the second largest in the cross section and is 12-20%. If this state is not included in the model the likelihood value changes by a large amount: $\delta L = 245$ and can not be compensated by adding other waves. It decays mainly into the broad S-wave contributions: σ and $\sigma * s$ terms. The decays into $f_2(1275)\pi$ and $f_0(980)\pi$ are found to be negligeable. This feature makes it difficult to define precisely the mass position of the resonance which changes when either a nonresonant contribution or the $\pi(1800)$ state is introduced in the fit. However the contribution of the resonance in the total cross section changes very little in different fits and the product of the $\gamma\gamma$ width times the branching ratio into $\pi^+\pi^-\pi^0$ can be measured.

- $a_2(1750)$

  This state was already observed in the previous analysis of the L3 data [3]. An appreciable contribution from this state, 8-11%, is present also in this analysis. If the resonance is not included in the fit the likelihood becomes worse, by $\delta L = 95$ and there are visible discrepancies in the description of some variables. The ratio between $^5S_2$ and $^1D_2$ states is found to be: $R = 0.75 \pm 0.20$. This almost coincides with theoretical calculations performed in [16] for the first radial recurrence of $a_2(1320)$.

- **$\pi(1800)$ and π_2 state**

  The fit of the data of the year 1998 analysed so far shows an improvement of $\delta L = 20$ when the $\pi(1800)$ state is introduced with mass and width taken from PDG [13]. The decay of this state to $f_0\pi$ and $f_2\pi$ also corresponds to the observations in other experiments. However this state is not seen in a preliminary analysis of the other data samples from the years 1999 and 2000. It needs still more work to be clarified.

  In the fit quite an appreciable 2^{-+} signal is found in the mass region 1700-1950 MeV. This signal can be partly related to the $\pi_2(1670)$. Further study on higher statistics sample is needed.

References

[1] JADE Coll. J.E. Olsson: Proc. V Int. Conf. on Two-Photon Physics, Aachen 1983 ed. Ch. Berger (Springer, Berlin 1983);
CELLO Coll. H.J. Behrend et al.: Phys.Lett. 114B 378 (1982); Phys.Lett. 125 518 (1983);
Pluto Coll. Ch. Berger et al.: Phys. Lett. 149B 427 (1984);
TASSO Coll. M. Althoff et al.: Z. Phys. C 31 537 (1986);
MARK2 Coll. F. Butler et al.: Phys Rev. D 42 1368 (1990);

MD1 Coll. S.E. Baru et al.: Z. Phys. C 48 581 (1990);

[2] ARGUS Coll. E. Kriznic: Il Nuovo Cimento 107 A N. 11 (1994);
ARGUS Coll. H. Albrecht et al.: Z. Phys C 74 469 (1997).

[3] L3 Coll. M.Acciari et al.: Phys. Lett. B 413 (1997) 147.

[4] L. Landau, Dokl. Akad. Nauk. SSSR 60 (1948) 207;
C.N. Yang, Phys. Rev. 77 (1950) 242.

[5] G.A. Schuler et al., Nucl. Phys. B 523 (1998) 423.

[6] V.M. Budnev et al.:Phys. Rep. 15 (1975) 181.

[7] R.Brun et al., GEANT 3.15 preprint CERN DD/EE/84-1 (Revised 1987).

[8] H. Fesefeldt, RWTH Aachen report PITHA 85/2 (1985).

[9] L3 Coll. B. Adeva et al.: Nucl. Instr. Meth. A289 35 (1990).

[10] P. Bene et al., Nucl. Inst. Meth. A 306 (1991) 150;
D. Haas et al,. Nucl. Inst. Meth. A 420 (1999) 101.

[11] M. Diehl, T. Gousset, B.Pire, Phys. Rev. D 62, 073014 (2000).

[12] V.V. Anisovich, D.V. Bugg, A.V. Sarantsev and B.S. Zou: Phys.Atom.Nucl 57 (1994) 1595.

[13] Review of Particle Physics, Phys. Rev. C 15 (2000).

[14] D.V. Bugg, B.S. Zou, A.V. Sarantsev: Nucl.Phys. B 471 (1996) 59.

[15] By V.V. Anisovich, Yu.D. Prokoshkin and A.V. Sarantsev. Phys.Lett. B 389 (1996) 388, hep-ph/9610414.

[16] By A.V. Anisovich, V.V. Anisovich, M.A. Matveev, V.N. Nikonov: in preparation.

J^{PC}	Resonance	M (MeV)	Γ(MeV)	$\Gamma_{\gamma\gamma} Br$(keV)
2^{++}	$a_2(1320)$	1307	130	0.71 ± 0.04
2^{++}	$a_2(1750)$	1730	310	0.26 ± 0.05
0^{-+}	$\pi(1300)$	1310	340	1.6 ± 0.2
0^{-+}	$\pi(1800)$	1840	320	
2^{-+}	$\pi_2(1670)$	1670	260	

Table 1: Preliminary results from the spin-parity analysis. The resonance mass and width obtained in the fit are indicated. For $\pi_2(1670)$ the mass and width are fixed to the world average value. The partial width $\Gamma_{\gamma\gamma}$ times the the branching ratio to $\pi^+\pi^-\pi^0$ is given with the statistical error only.

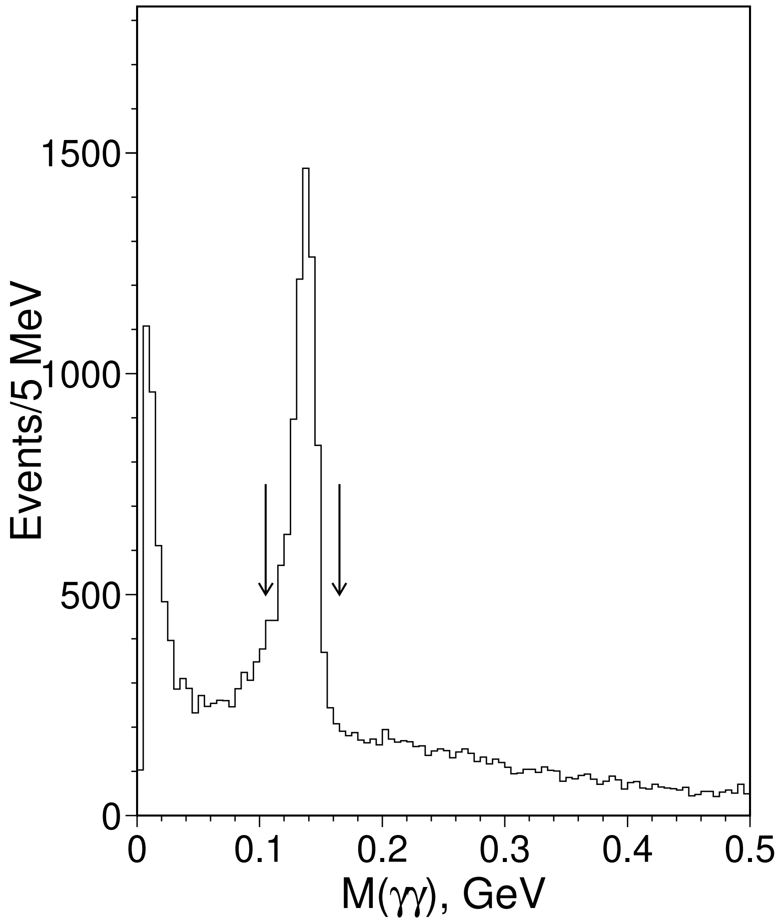

Figure 1: Mass of the two photons for $e^+e^- \to e^+e^-\pi^+\pi^-\pi^0$ events. The arrows indicate the cuts used to select the π^0 events.

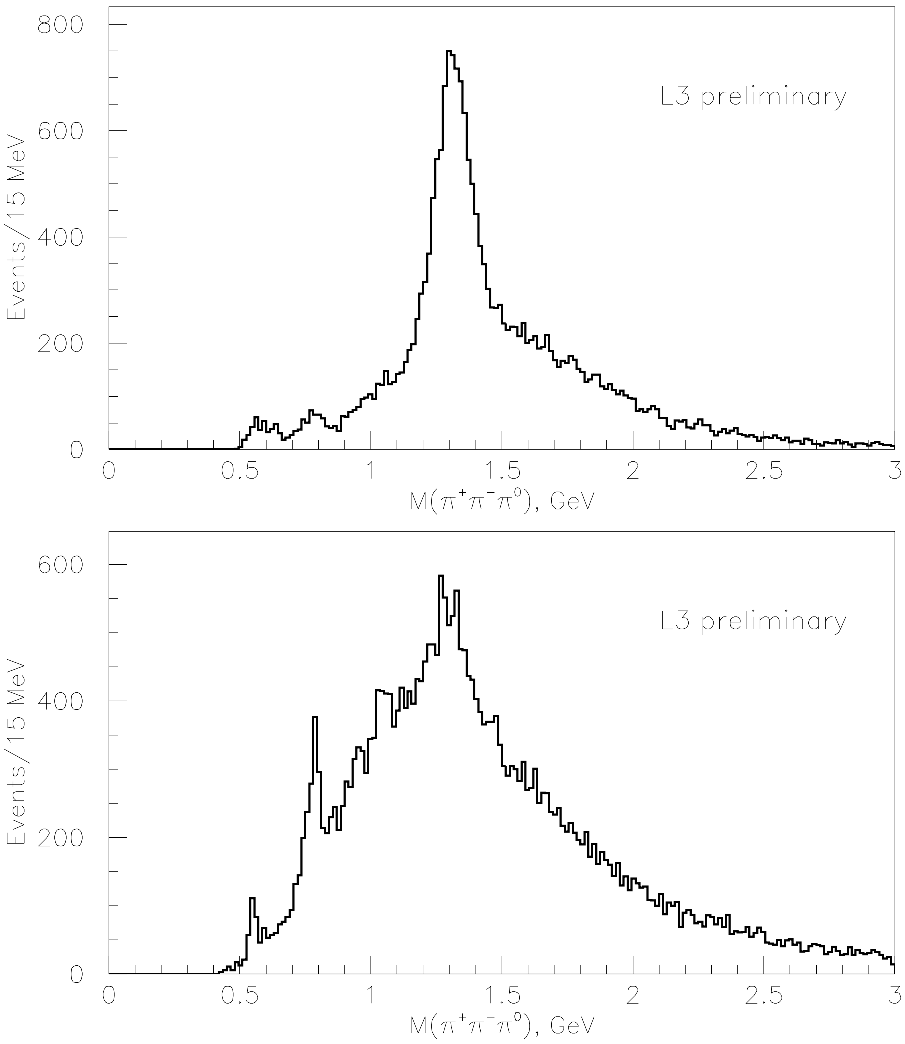

Figure 2: The $\pi^+\pi^-\pi^0$ mass spectra for $(\Sigma\vec{p}_T)^2 \leq 0.02GeV^2$ (upper plot) and $(\Sigma\vec{p}_T)^2 \geq 0.02GeV^2$ (lower plot).

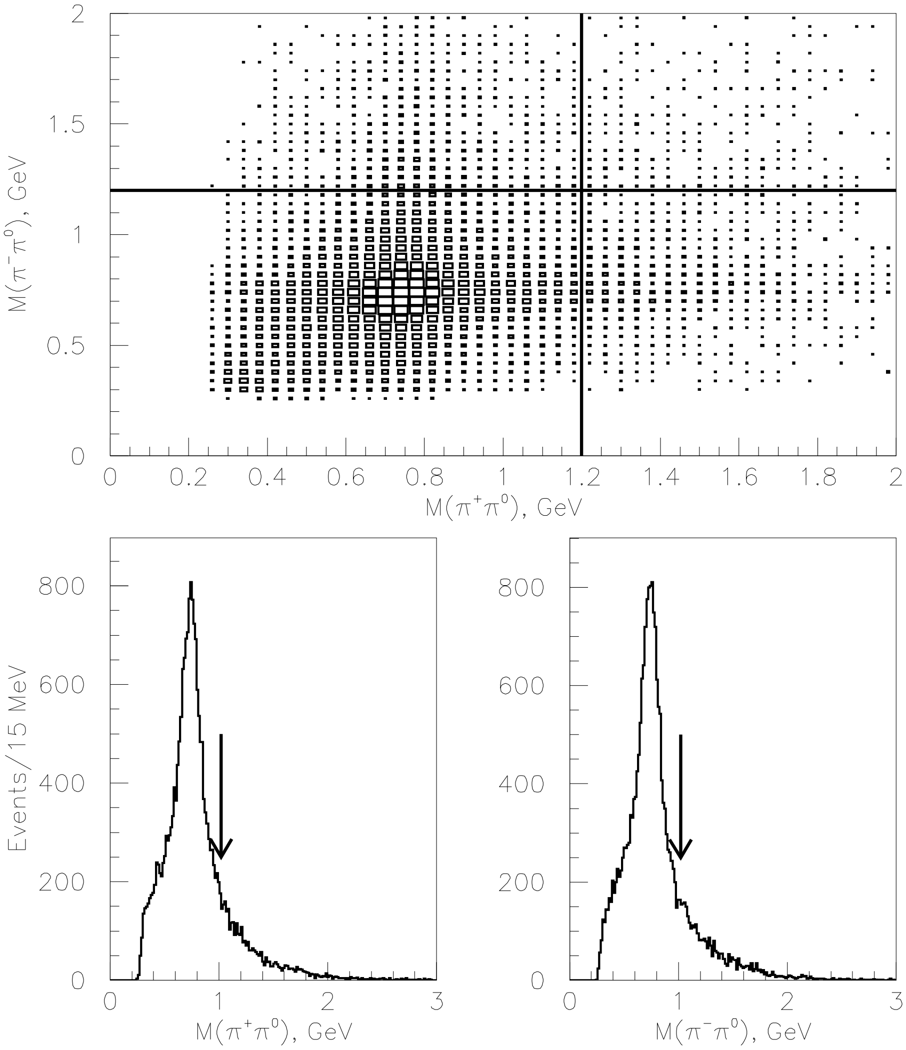

Figure 3: Two dimensional plot $M(\pi^+\pi^0) vs. M(\pi^-\pi^0)$ for the full data sample of $e^+e^- \rightarrow e^+e^-\pi^+\pi^-\pi^0$ events taken at $183 \leq \sqrt{s} \leq 209$GeV with a $(\Sigma\vec{p}_T)^2 \leq 0.02 GeV^2$. In the $\pi^\pm\pi^0$ mass projections the cut which selects the $a_2(1320)$ is indicated.

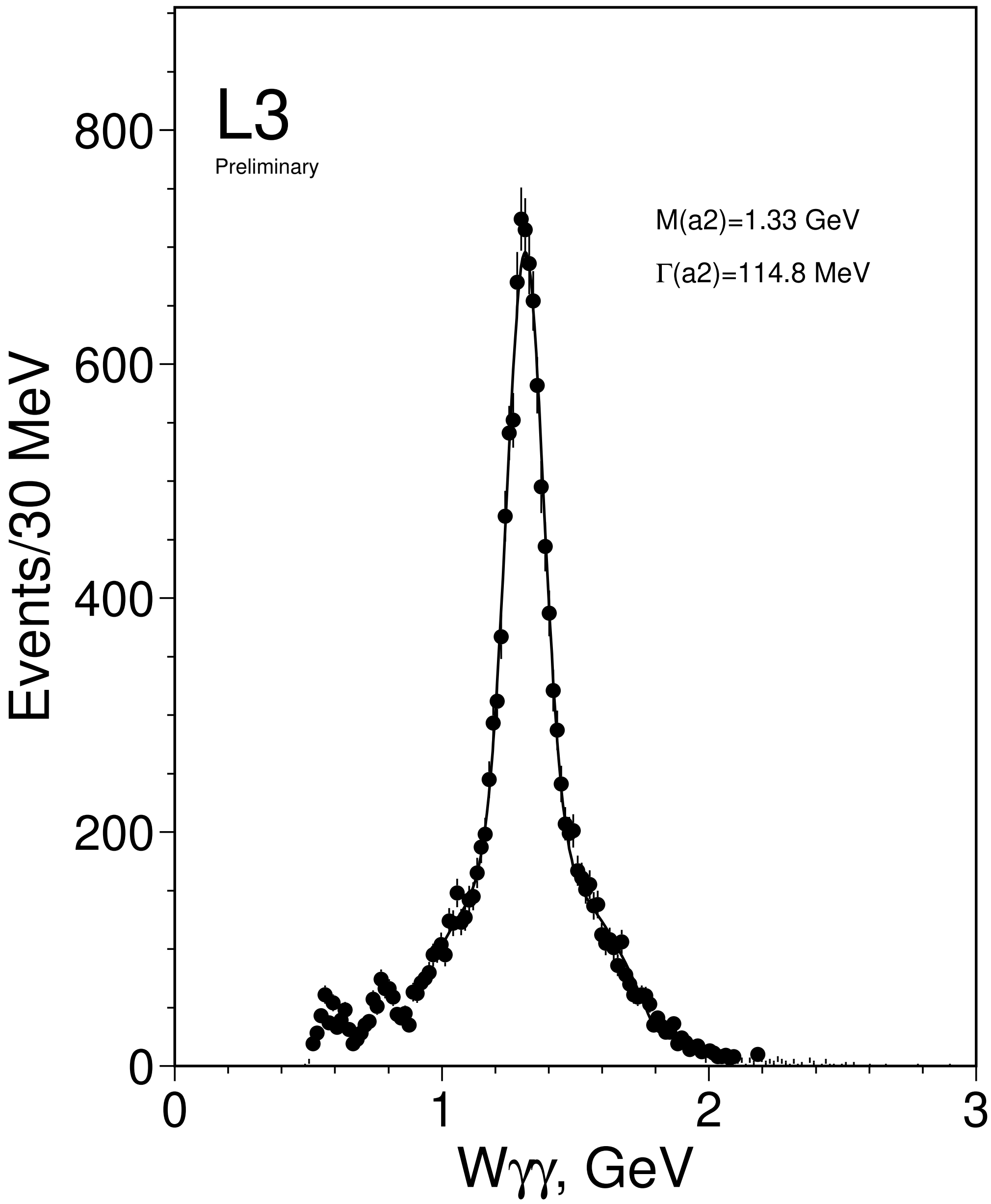

Figure 4: $\pi^+\pi^-\pi^0$ mass projection and the fit to a_2 mass and width.

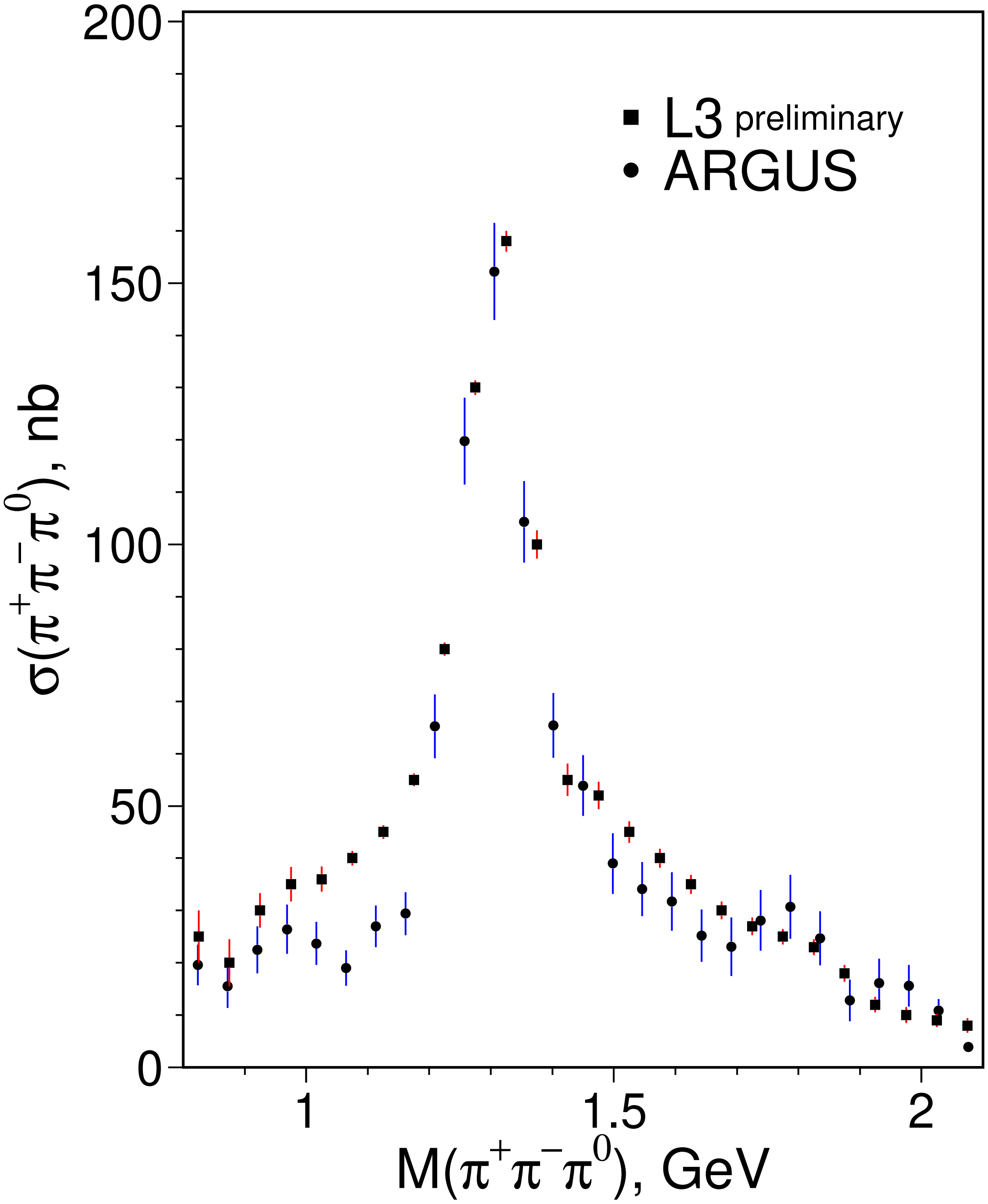

Figure 5: Cross section for $\gamma\gamma \to \pi^+\pi^-\pi^0$ measured at $183 \leq \sqrt{s} \leq 209$GeV compared to the ARGUS [1,2] results at $\sqrt{=}$10.4 GeV.

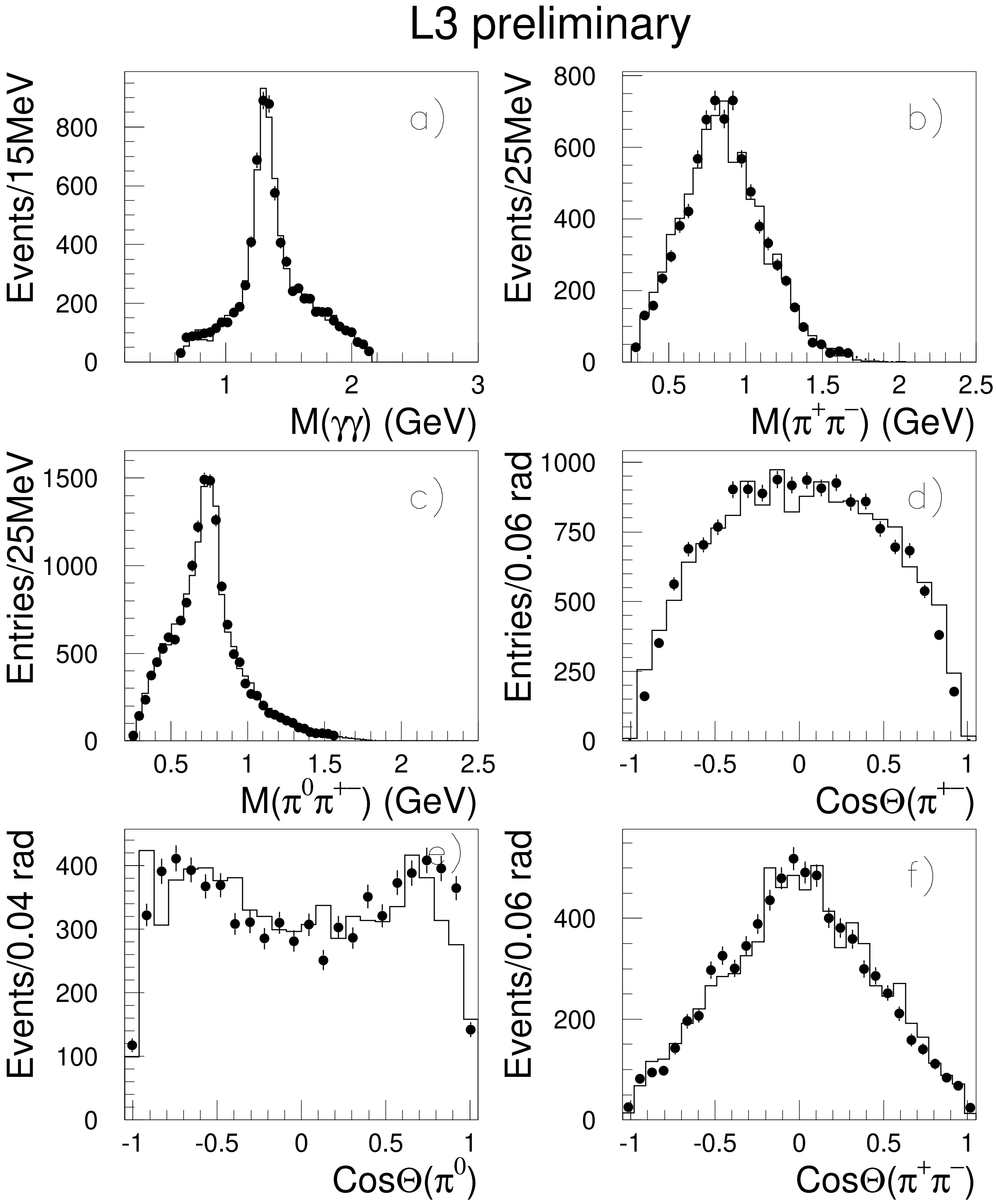

Figure 6: The data of the year 1998 (dots with error bar) for $0.65 \leq M(\gamma\gamma) \leq 2.15$ compared to the maximum likelihood fit results (histogram) described in text. The distribution of a) the $\pi^+\pi^-\pi^0$ mass, b) the $\pi^+\pi^-$ mass, c) the $\pi^0\pi$ mass, d) the angular distribution of the $\pi^\pm$ in the $\gamma\gamma$ c.m.s. e) the angular distribution of the π^0 in c.m.s. of $\gamma\gamma$ system and f) the angular distribution of charge pion in $\pi^+\pi^-$ c.m.s. system .

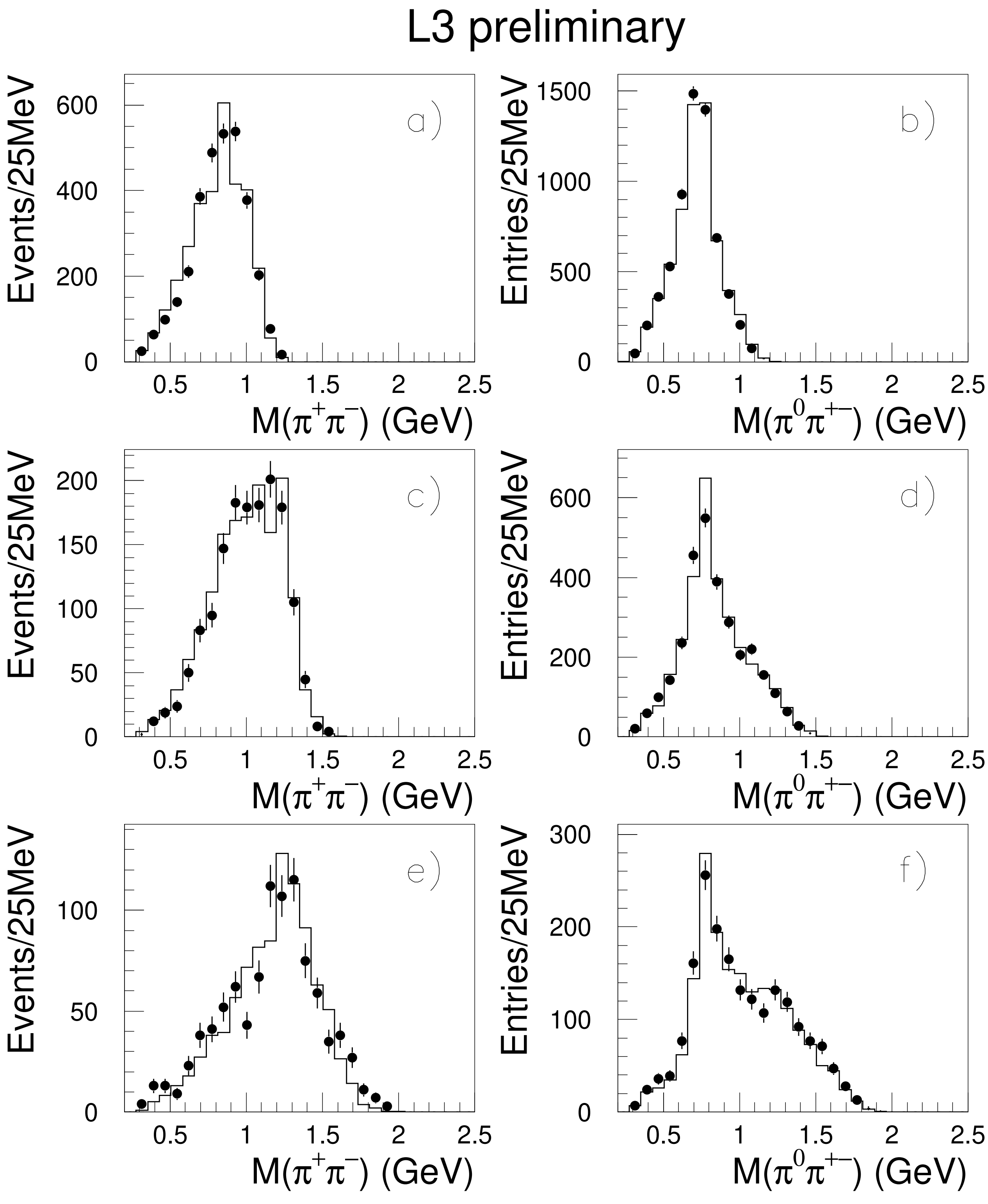

Figure 7: The distribution of $\pi^+\pi^-$ mass (left column) and $\pi^0\pi^\pm$ mass (right column) at different energy intervals of two-photon mass. a)b) for $1200MeV \leq M_{\gamma\gamma} \leq 1400MeV$ c)d) for $1500MeV \leq M_{\gamma\gamma} \leq 1700MeV$ e)f) for $1700MeV \leq M_{\gamma\gamma} \leq 1900MeV$.

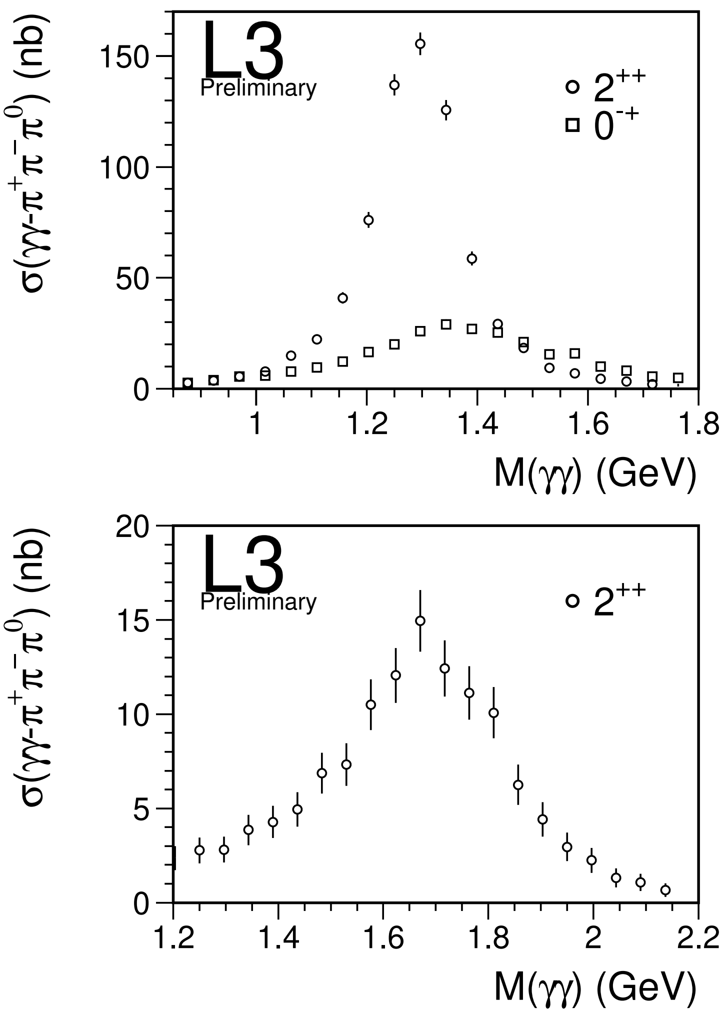

Figure 8: The contributions of the resonances to the cross section $\gamma\gamma \to \pi^+\pi^-\pi^0$ obtained by the energy dependent partial wave analysis: a) the contributions of $a_2(1320)$ and $\pi(1300)$ b) the contribution of $a_2(1730)$.